

# Fast finite-time backstepping controller for a quadrotor UAV under state constraints

Mung Xuan Nguyen<sup>1,\*</sup>, Lanh Le Thanh<sup>1</sup>, The Mich Nguyen<sup>2</sup>

<sup>1</sup>*Faculty of Technology, Dong Nai Technology University, Nguyen Khuyen, Bien Hoa, Dong Nai, Viet Nam*

<sup>2</sup>*Department of Vehicle and Energy Conversion Engineering, School of Mechanical Engineering, Hanoi University of Science and Technology, 1 Dai Co Viet, Hai Ba Trung, Ha Noi, Viet Nam*

\*Emails: [nguyexuanmung@dnvu.edu.vn](mailto:nguyexuanmung@dnvu.edu.vn)

Received: 28 February 2023; Accepted for publication: 12 May 2023

**Abstract.** Quadrotors have gained popularity in a wide range of applications. In this paper, a new approach for solving the tracking control problem of quadrotors with full-state constraints is presented. The proposed method involves a backstepping control scheme integrated with a fast finite-time filter. First, necessary state transformations are performed to support the design of the finite-time filter and controller. Next, the controller is formulated based on the backstepping technique. All the state constraints are taken into consideration in the controller. However, it is well-known that the backstepping control design can lead to the “explosion of complexity” when calculating time derivatives of certain nonlinear functions. Therefore, the proposed filter comes to provide a solution for estimating the time derivatives with the estimation errors converging to zero in finite time. The closed-loop system’s finite-time stability is rigorously proved using the Lyapunov theory, despite the state constraints. Simulation results demonstrate the feasibility and efficacy of the proposed method.

*Keywords:* Quadrotor, backstepping, finite-time, state constraint, tracking control.

*Classification numbers:* 5.10.2, 5.3.7.

## 1. INTRODUCTION

Quadrotor unmanned aerial vehicles (UAVs) have become a subject of great interest in the research community, primarily because of their unique capabilities, such as vertical taking off and landing, a wide range of flight capabilities, from hovering to cruising, the ability to fly at low altitudes, and their agility in tightly constrained environments [1, 2]. In practical applications, it is often necessary for these quadrotors to accurately track a given trajectory in a timely manner. However, due to their coupled nonlinear dynamics, parameterized uncertainties, and external disturbances [3], controlling quadrotors remains a challenging task.

Linear control methods, including the proportional-integral-derivative (PID) technique [4], linear quadratic regulation (LQR) [5], and robust H-infinity control [6], have been widely used

in quadrotor control system design and have advantages in project realization. However, their performance degrades when quadrotors leave their designed trim points or perform aggressive maneuvers. To address these shortcomings, various nonlinear control approaches have been introduced, such as dynamic inverse [7], backstepping (BS) [8], model predictive control [9], singular perturbation theory [10], and sliding mode (SM) control [11]. Recursive BS, which is a powerful Lyapunov-based tool, is typically used as a baseline controller for quadrotors due to the cascaded structure of their dynamics. The BS framework provides two significant benefits: 1) it accommodates nonlinearities and avoids wasteful cancelations [12], and 2) it allows several flight modes, such as position hold, loiter, and stabilized flight modes, to be integrated into the vehicle's control system due to the hierarchical scheme of BS.

The traditional BS method is known to have several issues. One such problem is the "explosion of complexity" caused by repeated differentiation of certain nonlinear functions, which is especially evident in high-order nonlinear systems. Moreover, traditional BS lacks a guarantee of robustness against perturbations. To address these limitations, researchers have proposed several adaptive control techniques for quadrotors. For instance, in [13], a radial basis function neural approximator was introduced to estimate and compensate for perturbations. Meanwhile, an immersion and invariance-based adaptive controller was developed in [14] for quadrotors that can handle uncertain inertial parameters, albeit in a relatively slow and indirect manner. More recently, the work in [15] proposed an active disturbance rejection control that employs a disturbance observer (DO) to estimate and compensate for lumped unknown disturbances in real-time. This approach has been further refined in [16], which combines command filtering with a DO to accurately track virtual control signals and attenuate the effect of disturbing forces and moments. To achieve highly precise and fast tracking, under the presence of uncertainties and disturbances, the use of dynamic surface control and an extended state observer within a DO-based control framework was presented in [17]. Overall, the application of these adaptive techniques can help achieve accurate tracking for quadrotors.

Our work aims to enhance the performance of the BS control by introducing finite-time convergence properties. Finite-time controllers provide a faster transient response and higher precision compared to asymptotic stability controllers when states are close to the equilibrium point [18]. We apply fraction powers of the tracking errors to achieve finite-time convergence and employ finite-time filters to estimate the time derivatives of virtual control inputs, thereby avoiding the "explosion of complexity" phenomenon. Simulation results demonstrate the effectiveness of the finite-time controller, which, to the best of our knowledge, has not been tested for quadrotor tracking control before.

Our work presents several contributions:

- First, we propose a multivariable composite finite-time BS framework that introduces fractional powers of tracking errors to improve convergence near the trim point. We estimate derivatives of virtual control inputs (virtual commands) using finite-time filters to avoid the "explosion of complexity."
- Second, we solve the tracking control problem of quadrotors that are subject to state constraints using our proposed finite-time BS. Our method guarantees finite-time convergence of tracking errors.
- Third, we prove the finite-time stability of the closed-loop system based on the finite-time Lyapunov theory. We demonstrate the effectiveness of our proposed control law through numerical simulations.

The organization of this paper is as follows. In Section 2, the dynamic model of the quadrotor is presented, and the control problem is defined. Section 3 introduces the finite-time controller design and provides a stability analysis of the closed-loop system. Simulation results are presented and discussed in Section 4. Finally, Section 5 concludes the paper.

## 2. PROBLEM STATEMENT AND PRELIMINARIES

### 2.1 Quadrotor dynamics model

In this section, we provide a brief summary of the quadrotor dynamics model, which was previously presented in many existing studies [1 - 4].

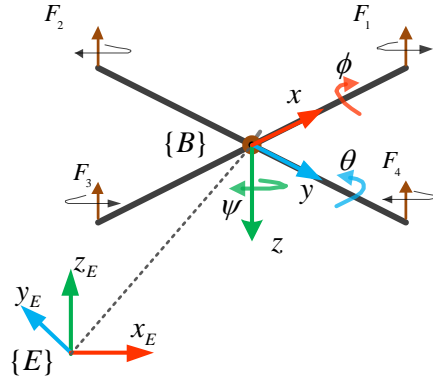


Figure 1. Quadrotor configuration. Motors 1 and 3 rotate counterclockwise while the other two motors rotate clockwise.

Let  $\phi$ ,  $\theta$ , and  $\psi$  denote three Euler angles roll, pitch, and yaw, respectively, in an earth-fixed frame  $\{E\}$  (Figure 1);  $J_x$ ,  $J_y$ , and  $J_z$  represent the moments of inertia about the  $x$ ,  $y$ , and  $z$  axes, respectively, in the body-fixed frame  $\{B\}$ ; and  $p$ ,  $q$ , and  $r$  denote the quadrotor's angular velocity about the  $x$ ,  $y$ , and  $z$  axes, respectively, in  $\{B\}$ . The quadrotor's attitude dynamics model can be described as follows.

$$\begin{cases} \dot{p} = \left( \frac{J_y - J_z}{J_x} \right) qr + \frac{1}{J_x} u_\phi \\ \dot{q} = \left( \frac{J_z - J_x}{J_y} \right) rp + \frac{1}{J_y} u_\theta \\ \dot{r} = \left( \frac{J_x - J_y}{J_z} \right) pq + \frac{1}{J_z} u_\psi \end{cases} \quad (1)$$

The time derivative of the attitude  $[\phi, \theta, \psi]^T$  can be expressed in terms of the angular velocity  $[p, q, r]^T$  as follows.

$$\begin{bmatrix} \dot{\phi} \\ \dot{\theta} \\ \dot{\psi} \end{bmatrix} = \begin{bmatrix} 1 & \sin \phi \tan \theta & \cos \phi \tan \theta \\ 0 & \cos \phi & -\sin \phi \\ 0 & \frac{\sin \phi}{\cos \theta} & \frac{\cos \phi}{\cos \theta} \end{bmatrix} \begin{bmatrix} p \\ q \\ r \end{bmatrix} \quad (2)$$

Linearizing (2) near the quadrotor's hovering point, where  $\phi = \phi_{hv} = 0$  and  $\theta = \theta_{hv} = 0$ , yields:

$$\begin{bmatrix} \dot{\phi} \\ \dot{\theta} \\ \dot{\psi} \end{bmatrix} = \begin{bmatrix} 1 & 0 & 0 \\ 0 & 1 & 0 \\ 0 & 0 & 1 \end{bmatrix} \begin{bmatrix} p \\ q \\ r \end{bmatrix} \quad (3)$$

In other words, (3) can be expressed as  $[\dot{\phi}, \dot{\theta}, \dot{\psi}]^T = [p, q, r]^T$ . Thus, (1) can be rewritten as follows.

$$\begin{cases} \ddot{\phi} = \left( \frac{J_y - J_z}{J_x} \right) \dot{\theta} \dot{\psi} + \frac{1}{J_x} u_\phi \\ \ddot{\theta} = \left( \frac{J_z - J_x}{J_y} \right) \dot{\phi} \dot{\psi} + \frac{1}{J_y} u_\theta \\ \ddot{\psi} = \left( \frac{J_x - J_y}{J_z} \right) \dot{\phi} \dot{\theta} + \frac{1}{J_z} u_\psi \end{cases} \quad (4)$$

where,  $u_i$  ( $i = \phi, \theta, \psi$ ) denotes the control inputs which are generated by the quadrotor's motor thrust forces,  $F_j = c_t \omega_j^2$ , ( $j = 1, 2, 3, 4$ ), as follows.

$$\begin{cases} u_\phi = l(F_2 - F_4) \\ u_\theta = l(F_1 - F_3) \\ u_\psi = c_d(F_1 + F_3 - F_2 - F_4) \end{cases} \quad (5)$$

where,  $\omega_j$  is the speed of motor  $j$ ;  $c_t$  and  $c_d$  the thrust and drag coefficients, respectively;  $l$  the arm length of the quadrotor.

It is seen in (4) that the dynamics of the roll, pitch, and yaw angles are in similar form to each other. Therefore, the following representative system (6) will be considered, and the control design and verification process of this representative system can be applied directly to that of the roll, pitch, and yaw angle dynamics.

$$\begin{cases} \dot{x}_{1i} = x_{2i} \\ \dot{x}_{2i} = b_i u_i + g_i \\ y_i = x_{1i} \end{cases} \quad (6)$$

where,  $x_{1i} = \phi, \theta, \psi$  and  $x_{2i} = \dot{\phi}, \dot{\theta}, \dot{\psi}$ ;  $x_i = [x_{1i}, x_{2i}]^T$  is the new state variables;

$b_i = 1/J_x, 1/J_y, 1/J_z$ ;  $u_i = u_\phi, u_\theta, u_\psi$ ,  $g_i = \left( \frac{J_y - J_z}{J_x} \right) \dot{\theta} \dot{\psi}$ ,  $\left( \frac{J_z - J_x}{J_y} \right) \dot{\phi} \dot{\psi}$ ,  $\left( \frac{J_x - J_y}{J_z} \right) \dot{\phi} \dot{\theta}$ ; and  $y_i$  is the

output. Here, it is worth noting that all the states suffer from state constraints, that is:

$$\begin{cases} -k_{11i} < x_{1i} < k_{12i} \\ -k_{21i} < x_{2i} < k_{22i} \end{cases}, k_{1ji}, k_{2ji} > 0 \quad (7)$$

For a typical quadrotor, the values of the upper and lower limits of the attitude are  $k_{11i} = k_{12i} = \frac{\pi}{2}$  for the roll and pitch angles, and  $k_{11i} = k_{12i} = \pi$  for the yaw angle.

## 2.2 Control objective

The overall control scheme consists of position and attitude controllers (Figure 2). The quadrotor tracking control problem involves position tracking and attitude tracking. However, attitude tracking control plays a key role in improving the whole system's tracking performance due to two major reasons. First, as can be seen in Figure 2, the position controller generates the desired roll and pitch angles which can only be tracked if the attitude tracking controllers are designed properly. Second, every unexpected change in the system states can be quickly compensated by the attitude tracking controller as the attitude dynamics is much faster than the position dynamics.

From the above observation, this paper aims to propose a novel fast finite-time backstepping attitude control algorithm to drive the quadrotor, under state constraints (7), to track the desired attitude  $\phi_d, \theta_d, \psi_d$ .

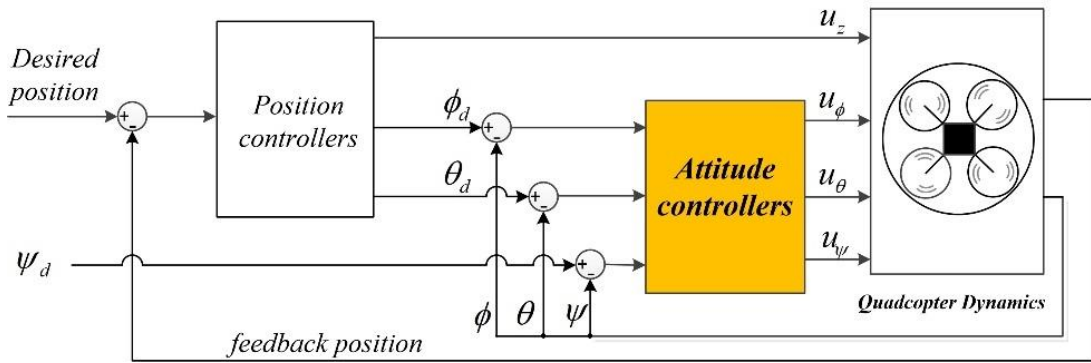


Figure 2. Full quadrotor controller scheme. The proposed algorithm is applied to the attitude controllers, which play key roles in the system's tracking control performance.

The following assumption, lemmas, and proposition are used in our control design and stability analysis, which will be presented in Section 3.

**Assumption 1.** The desired attitude  $y_{id}$  and its time derivative  $\dot{y}_{id}$  are continuous and bounded.

**Lemma 1** [19]. Let  $\varsigma_1, \varsigma_2, \dots, \varsigma_q \in \mathbb{R}^+$ , if  $p > 0$ , then the following holds.

$$\max\{q^{p-1}, 1\}(\varsigma_1^p + \varsigma_2^p + \dots + \varsigma_q^p) \geq (\varsigma_1 + \varsigma_2 + \dots + \varsigma_q)^p.$$

**Lemma 2** [20]. (Finite-Time Uniformly Ultimately Boundedness): Consider the following system.

$$\dot{x}(t) = f(x(t)), f(0) = 0, x \in \mathbb{R}^n$$

Suppose there is a Lyapunov function  $V(x)$ , positive constants  $p \in (0, 1)$ ,  $\alpha > 0$  and  $\beta > 0$ , such that  $\dot{V}(x) \leq -\alpha V^p(x) + \beta$ . Then, the state  $x(t)$  is uniformly ultimately finite-time stable. It means that the state can converge to a region of the equilibrium point in a finite time.

**Lemma 3** [21]: Consider the system  $\dot{x} = f(x)$ ,  $f(0) = 0$ ,  $x \in \mathbb{R}^n$ , if there is a positive-definite continuous function  $V(x) : \mathbb{R}^n \rightarrow \mathbb{R}$ , makes  $\dot{V}(x) \leq -\alpha_1 V^{\beta_1}(x) - \alpha_2 V^{\beta_2}(x)$ , where

$\alpha_1, \alpha_2 > 0, 0 < \beta_1 < 1, \beta_2 > 1$ . Then, the system is stable in a finite-time, and the convergence time  $T_c$  satisfies:  $T_c \leq 1/[\alpha_1(1 - \beta_1)] + 1/[\alpha_2(\beta_2 - 1)]$ .

**Proposition 1.** For a function  $f(x) = -\alpha_1 x^{2\beta_1} - \alpha_2 x^{2\beta_2} - \alpha_3 x^2$ , with  $0 < \beta_1 < 1, \beta_2 > 1$  and tunable parameters  $\alpha_1, \alpha_2 > 0$ , there always exist positive numbers  $\gamma_1$  and  $\gamma_2$  such that  $f(x) \leq -\gamma_1 x^{2\beta_1} - \gamma_2 x^{2\beta_2}$ .

### 3. METHODOLOGY

The control system is designed in this section by integrating a fast finite-time filter into the backstepping control technique. The filter aims to circumvent the ‘‘explosion of complexity’’ problem. Before moving on to the design, some state transformations are conducted. For the sake of simplicity in control design and closed-loop system’s stability analysis, the following state transformations are performed.

#### 3.1. State transformations

$$\xi_{ji} = \frac{x_{ji}}{(k_{j1i} + x_{ji})(k_{j2i} - x_{ji})} = \frac{x_{ji}}{\sigma_{ji}}, \quad i = \phi, \theta, \psi; \quad j = 1, 2 \quad (8)$$

and

$$\mu_{ji} = \frac{k_{j1i}k_{j2i} + x_{ji}^2}{\sigma_{ij}^2}, \quad \mu_{id} = \frac{k_{11i}k_{12i} + y_{id}^2}{\sigma_{id}^2} \quad (9)$$

where,  $\sigma_{ji} = (k_{j1i} + x_{ji})(k_{j2i} - x_{ji})$ ,  $\sigma_{id} = (k_{11i} + y_{id})(k_{12i} - y_{id})$ .

With the above state transformations, the tracking errors are defined as follows.

$$e_{1i} = \xi_{1i} - v_{0i} \quad (10)$$

and

$$e_{2i} = \xi_{2i} - \hat{v}_{1i} \quad (11)$$

where,  $v_{0i} = y_{id} / [(k_{11i} + y_{id})(k_{12i} - y_{id})]$  and  $\hat{v}_{1i}$  is the filtered signal provided by the filter, which will be described in next subsection.

#### 3.2. Fast finite-time backstepping controller

*Step 1.* From (6), (8), (9) and (10), the time derivative of  $e_{1i}$  can be obtained as:

$$\dot{e}_{1i} = \mu_{1i}x_{2i} - \mu_{id}\dot{y}_{id} \quad (12)$$

A virtual control input,  $v_{1i}$ , for (12) is designed as:

$$v_{1i} = \frac{1}{\mu_{1i}}(\mu_{id}\dot{y}_{id} - \gamma_{11i}\text{sig}^{\lambda_{1i}}e_{1i} - \gamma_{12i}\text{sig}^{\lambda_{2i}}e_{1i}) \quad (13)$$

with  $\gamma_{11i}, \gamma_{12i} > 0$  and  $0 < \lambda_{1i} < 1, \lambda_{2i} > 1$ .

Then, the derivative of  $e_{2i}$  is

$$\dot{e}_{2i} = \dot{\xi}_{2i} - \dot{\hat{v}}_{1i} \quad (14)$$

where,  $\hat{v}_{1i}$  denotes the estimated value of  $v_{1i}$ , which is obtained through the following finite-time filter to avoid the ‘‘explosion of complexity’’ in the calculation of  $\dot{v}_{1i}$ .

$$\tau_i \dot{\hat{v}}_{1i} = \text{sig}^{\lambda_{1i}} \left( \frac{v_{1i}}{\sigma_{2i}} - \hat{v}_{1i} \right) + \text{sig}^{\lambda_{2i}} \left( \frac{v_{1i}}{\sigma_{2i}} - \hat{v}_{1i} \right) + \text{sig}^{\lambda_{3i}} \left( \frac{v_{1i}}{\sigma_{2i}} - \hat{v}_{1i} \right) \quad (15)$$

with  $\tau_i$  being the filter parameter,  $\text{sig}^\lambda(x) = \text{sgn}(x)|x|^\lambda$ , and  $\lambda_{3i}$  is defined as

$$\lambda_{3i} = \begin{cases} \min\{\lambda_{1i}, |e_{fi}|\}, & |e_{fi}| < 1 \\ \max\{\lambda_{2i}, |e_{fi}|\}, & |e_{fi}| \geq 1 \end{cases} \quad (16)$$

where,  $e_{fi} = \hat{v}_{1i} - \frac{v_{1i}}{\sigma_{2i}}$  is the estimate error. Thus, we have

$$\xi_{2i} = e_{2i} - \hat{v}_{1i} = e_{2i} + e_{fi} + \frac{v_{1i}}{\sigma_{2i}} \quad (17)$$

Then, from (12), (13), and (15), we have

$$\dot{e}_{1i} = \mu_{1i}\sigma_{2i}(e_{2i} + e_{fi}) - \gamma_{11i}\text{sig}^{\lambda_{1i}}e_{1i} - \gamma_{12i}\text{sig}^{\lambda_{2i}}e_{1i} \quad (18)$$

*Step 2.* From (6) and (14), we have

$$\dot{e}_{2i} = \mu_{2i}(b_i u_i + g_i) - \dot{\hat{v}}_{1i} \quad (19)$$

The actual control input is designed as

$$u_i = \frac{1}{\mu_{2i}b_i} \left( \dot{\hat{v}}_{1i} - \mu_{2i}g_i - \gamma_{21i}\text{sig}^{\lambda_{1i}}e_{2i} - \gamma_{22i}\text{sig}^{\lambda_{2i}}e_{2i} \right) - \mu_{1i}\sigma_{2i}e_{1i} \quad (20)$$

Substituting (20) into (19) yields

$$\dot{e}_{2i} = -\gamma_{11i}\text{sig}^{\lambda_{1i}}e_{1i} - \gamma_{12i}\text{sig}^{\lambda_{2i}}e_{1i} - \mu_{1i}\sigma_{2i}e_{1i} \quad (21)$$

**Theorem 1.** Consider the quadrotor system (6) with full states being constrained as in (7), for a given time-varying desired attitude  $y_{id}$ , under the Assumption 1, the tracking errors  $e_{1i}$  and  $e_{2i}$  are ultimately bounded and asymptotically approach the origin in finite-time if the control input  $u_i$  is designed as in (20) and the virtual control law is formed as in (13) with the use of the filter in (15).

**Proof of Theorem 1.** Taking the tracking errors  $e_{1i}, e_{2i}$ , and the estimate error  $e_{fi}$  into consideration, let us choose a Lyapunov function candidate as follows.

$$V = \frac{1}{2}e_{1i}^2 + \frac{1}{2}e_{2i}^2 + \frac{1}{2}e_{fi}^2 = V_e + V_f \quad (22)$$

where,  $V_e = (e_{1i}^2 + e_{2i}^2)/2$  and  $V_f = e_{fi}^2/2$ . The time derivative of  $V$  is

$$\dot{V} = \dot{e}_{1i}e_{1i} + \dot{e}_{2i}e_{2i} + \dot{e}_{fi}e_{fi} = \dot{V}_e + \dot{V}_f \quad (23)$$

Following (18) and (21), one yields

$$\begin{aligned} \dot{V}_e &= e_{1i} \left[ \mu_{1i}\sigma_{2i}(e_{2i} + e_{fi}) - \gamma_{11i}\text{sig}^{\lambda_{1i}}e_{1i} - \gamma_{12i}\text{sig}^{\lambda_{2i}}e_{1i} \right] \\ &\quad + e_{2i}(-\gamma_{11i}\text{sig}^{\lambda_{1i}}e_{1i} - \gamma_{12i}\text{sig}^{\lambda_{2i}}e_{1i} - \mu_{1i}\sigma_{2i}e_{1i}) \\ &\leq - \left[ \gamma_{11i}(e_{1i}^2)^{\frac{\lambda_{1i}+1}{2}} + \gamma_{12i}(e_{1i}^2)^{\frac{\lambda_{2i}+1}{2}} + \gamma_{21i}(e_{2i}^2)^{\frac{\lambda_{1i}+1}{2}} + \gamma_{22i}(e_{2i}^2)^{\frac{\lambda_{2i}+1}{2}} \right] + e_{1i}\mu_{1i}\sigma_{2i}e_{fi} \\ &\leq - \left[ \gamma_{11i}(e_{1i}^2)^{\frac{\lambda_{1i}+1}{2}} + \gamma_{12i}(e_{1i}^2)^{\frac{\lambda_{2i}+1}{2}} + \gamma_{21i}(e_{2i}^2)^{\frac{\lambda_{1i}+1}{2}} + \gamma_{22i}(e_{2i}^2)^{\frac{\lambda_{2i}+1}{2}} \right] + \left( \frac{e_{1i}^2\mu_{1i}^2}{2} + \frac{\sigma_{2i}^2e_{fi}^2}{2} \right) \end{aligned} \quad (24)$$

From (15), the time derivative of  $e_{fi}$  can be obtained as

$$\dot{e}_{fi} = -\frac{1}{\tau_i} \left[ \text{sig}^{\lambda_i} e_{fi} + \text{sig}^{\lambda_{2i}} e_{fi} + \text{sig}^{\lambda_{3i}} e_{fi} \right] - d\left(\frac{v_{1i}}{\sigma_{2i}}\right) / dt \quad (25)$$

Thus, one yields:

$$\begin{aligned} \dot{V}_f &= -\frac{e_{fi}^{\lambda_i+1}}{\tau_i} - \frac{e_{fi}^{\lambda_{2i}+1}}{\tau_i} - \frac{e_{fi}^{\lambda_{3i}+1}}{\tau_i} + e_{fi} d\left(\frac{v_{1i}}{\sigma_{2i}}\right) / dt \\ &\leq -\frac{(e_{fi}^2)^{\frac{\lambda_i+1}{2}}}{\tau_i} - \frac{(e_{fi}^2)^{\frac{\lambda_{2i}+1}{2}}}{\tau_i} - \frac{(e_{fi}^2)^{\frac{\lambda_{3i}+1}{2}}}{\tau_i} + \frac{e_{fi}^2}{2} + \varepsilon_i^2 \end{aligned} \quad (26)$$

with  $\varepsilon > 0$  being the upper boundary (based on Assumption 1) satisfying  $\left| \frac{1}{\sqrt{2}} d\left(\frac{v_{1i}}{\sigma_{2i}}\right) / dt \right| \leq \varepsilon$ .

From (23), (24), and (26), according to Proposition 1, we have

$$\begin{aligned} \dot{V} &\leq -\gamma_{1i} (e_{1i}^2)^{\frac{\lambda_i+1}{2}} - \gamma_{12i} (e_{1i}^2)^{\frac{\lambda_{2i}+1}{2}} - \gamma_{2i} (e_{2i}^2)^{\frac{\lambda_i+1}{2}} - \gamma_{22i} (e_{2i}^2)^{\frac{\lambda_{2i}+1}{2}} + \frac{\mu_{1i}^2}{2} e_{1i}^2 \\ &\quad - \frac{(e_{fi}^2)^{\frac{\lambda_i+1}{2}}}{\tau_i} - \frac{(e_{fi}^2)^{\frac{\lambda_{2i}+1}{2}}}{\tau_i} - \frac{(e_{fi}^2)^{\frac{\lambda_{3i}+1}{2}}}{\tau_i} + \left(\frac{1}{2} + \frac{\sigma_{2i}^2}{2}\right) e_{fi}^2 + \varepsilon_i^2 \\ &\leq -\gamma_{1i} \left[ (e_{1i}^2)^{\frac{\lambda_i+1}{2}} + (e_{2i}^2)^{\frac{\lambda_i+1}{2}} + (e_{fi}^2)^{\frac{\lambda_i+1}{2}} \right] - \gamma_{2i} \left[ (e_{1i}^2)^{\frac{\lambda_{2i}+1}{2}} + (e_{2i}^2)^{\frac{\lambda_{2i}+1}{2}} + (e_{fi}^2)^{\frac{\lambda_{2i}+1}{2}} \right] + \varepsilon_i^2 \end{aligned} \quad (27)$$

where,  $\gamma_{1i}$  and  $\gamma_{2i}$  are positive constants which can be chosen appropriately according to Proposition 1.

Following Lemma 1, one can be obtained from (27) as

$$\dot{V} \leq -\frac{\gamma_{1i}}{3^{\frac{\lambda_i-1}{2}}} V^{\frac{\lambda_i+1}{2}} - \frac{\gamma_{2i}}{3^{\frac{\lambda_{2i}-1}{2}}} V^{\frac{\lambda_{2i}+1}{2}} + \varepsilon_i^2 \quad (28)$$

The inequality (28) indicates all the errors, including  $e_{1i}$ ,  $e_{2i}$ , and  $e_{fi}$ , are uniformly ultimately bounded (Lemma 2) and asymptotically approach the very small region close to the origin. This completes the proof.

*Remark 1.* The filter in (15) contributes to avoiding the ‘‘explosion of complexity’’ phenomenon in calculating the time derivative,  $\dot{\hat{v}}_{1i}$ , of the virtual control input  $v_{1i}$  in (13), which is required to compute the actual control input  $u_i$  in (20).

*Remark 2.* From (28), according to Lemma 3, it can be concluded that all the system states converge to the desired values in finite time  $T_c$ , which is bounded as follows.

$$T_c \leq \frac{2}{\gamma_{1i}(1-\lambda_i)} + \frac{2}{\gamma_{2i}(\lambda_{2i}-1)} \quad (29)$$

*Remark 3.* The scheme of the attitude controller is summarized in the following block diagram (Figure 3).

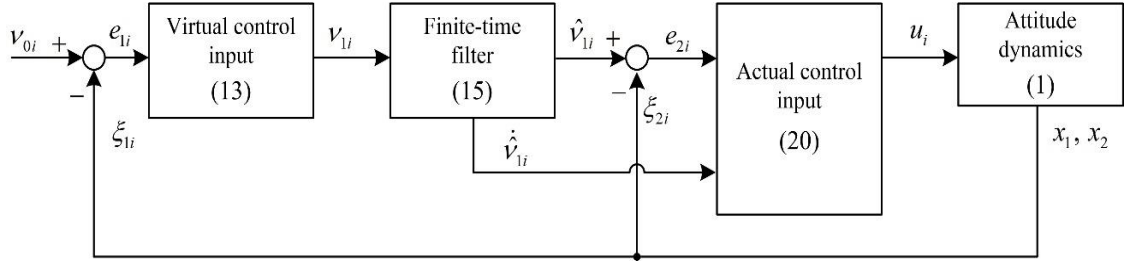


Figure 3. Block diagram of the quadrotor's attitude controller.

*Remark 4.* With the proposed controller, it is proved that the tracking errors,  $e_{1i}$  and  $e_{2i}$ , converge to zeros in finite-time. From the definitions of the tracking errors in (10) and (11), we have  $\xi_{1i} \rightarrow v_{0i}$  and  $\xi_{2i} \rightarrow \hat{v}_{1i}$ , with  $v_{0i}$  being calculated from the desired attitude (bounded), and  $\hat{v}_{1i}$  being the bounded output of the filter (15). Therefore, the denominators in (8), i.e.,  $(k_{11i} + x_{1i})(k_{12i} - x_{1i})$  and  $(k_{21i} + x_{2i})(k_{22i} - x_{2i})$ , do not reach zeros. In other words,  $x_{1i}$  does not reach its limits, i.e.,  $-k_{11i}$  and  $k_{12i}$ ; and  $x_{2i}$  does not reach its limits, i.e.,  $-k_{21i}$  and  $k_{22i}$ . Hence, that is the capability of our proposed method of dealing with the constraints.

Table 1. Quadrotor's dynamical parameters.

Parameter	Value	Unit
$[J_x, J_y, J_z]$	[0.012, 0.013, 0.022]	kg.m <sup>2</sup>
$l$	0.225	m
$c_t$	$10^{-6}$	N.s <sup>2</sup>
$c_d$	0.05	-
$[k_{11\phi}, k_{12\phi}]$	$[\pi/3, \pi/3]$	rad
$[k_{11\theta}, k_{12\theta}]$	$[\pi/3, \pi/3]$	rad
$[k_{11\psi}, k_{12\psi}]$	$[\pi/3, \pi/3]$	rad
$[k_{21\phi}, k_{22\phi}]$	$[\pi/2, \pi/2]$	rad/s
$[k_{21\theta}, k_{22\theta}]$	$[\pi/2, \pi/2]$	rad/s
$[k_{21\psi}, k_{22\psi}]$	$[\pi/2, \pi/2]$	rad/s

Table 2. Desired and initial attitude and parameters of the filters and controllers.

Parameter	Value	Unit
$\phi_d$	$-0.3; \frac{\pi}{6} \sin(\frac{\pi}{3}t) + 0.1 \sin(\pi t - \frac{\pi}{4})$	rad
$\theta_d$	$0.3; \frac{\pi}{12} \sin(\frac{\pi}{4}t + \frac{\pi}{3}) + 0.1 \sin(\pi t)$	rad
$\psi_d$	$-0.1; \frac{\pi}{4} \sin(\frac{\pi}{12}t)$	rad
$[\phi_0, \theta_0, \psi_0]$	[-0.1, 0.1, 0.1]	rad
$\tau_i$	0.01	s
$[\lambda_{1i}, \lambda_{2i}]$	[0.7, 1.5]	-
$[\beta_{11i}, \beta_{12i}, \beta_{21i}, \beta_{22i}]$	[1, 2, 10, 30]	-

*Remark 5.* The controllers and the filter in (13), (20), and (15) are designed based on model (4), which is obtained from (1) through a linearization near the hovering point, i.e.,  $\phi = 0$  and  $\theta = 0$ . Therefore, the quadrotor should be operated in an attitude range near this point to ensure the proposed controller functions properly. The further the quadrotor attitude is away from the hovering point, the more the control performance is degraded.

## 4. SIMULATION RESULTS AND DISCUSSIONS

This section demonstrates how our proposed method is effective in the tracking control of a quadrotor subject to full-state constraints. It is worth noting that, while the controller was designed based on (4), we utilized the dynamic model in (1) and the kinematic model in (2) to assess the closed-loop system's stability and confirm that our controller delivers satisfactory tracking control performance.

### 4.1. Simulation assumptions

The simulation was conducted assuming that the quadrotor's attitude is determined by an inertial navigation system (INS). The controllers were implemented in Matlab/Simulink with a sampling time of 0.0025 s, which corresponds to an operating frequency of 400 Hz. The quadrotor parameters and its state constraints used in the simulation (Table 1) were collected based on the parameters of a real F450 quadrotor platform [22], which is equipped with four 2312E motors and four 9450 propellers [23]. Table 2 lists the controller gains, initial conditions, and desired state values. By selecting fast, time-varying desired state values (Table 2), we illustrate the accuracy and rapidness of our new controller to track complex and fast-varying desired trajectories.

### 4.2. Simulation Results and Discussions

To evaluate the effectiveness of the proposed method, two test scenarios were conducted, namely the tracking of (i) step and (ii) complex and time-varying attitude references. The system performance corresponding to each scenario is examined and discussed in the following subsections.

#### 4.2.1. Tracking of step attitude references

In this scenario, the desired attitude is set as  $[-0.3, 0.3, -0.1]$  rad (Table 2). To generalize this test case, the quadrotor's initial states are set to non-zero, that is, the tracking flight is triggered at a non-hovering status. At  $t = 0$  s, the quadrotor's attitude tracking errors rapidly start converging to zero (Figure 4a). Simultaneously, the angular rate errors also see a quick convergence (Figure 4b). It is seen that the settling time (2 %) of all attitude angle tracking is about 2.5 seconds. Even though having a rapid convergence speed, the proposed controller does not require much control effort.

As per Figure 4c, all the control inputs do not exceed 1.0 N.m, which is already a pretty small value of control torque for a quadrotor like F450. Besides, to have such a fast response, a backstepping controller usually results in the chattering phenomenon in the control input. However, our controller input can be seen as chattering-free. Examining the filter's performance, as expected, the proposed filter provides a highly accurate and fast-converged estimate which is proved through the performance of the filter estimate errors (Figure 4d). Another aspect of being

validated is the state constraints (the dashed black lines in Figures 5a-b). It is clear that all states lie in the range of the constraints while exhibiting fast responses.

4.2.2. Tracking of complex and time-varying attitude references

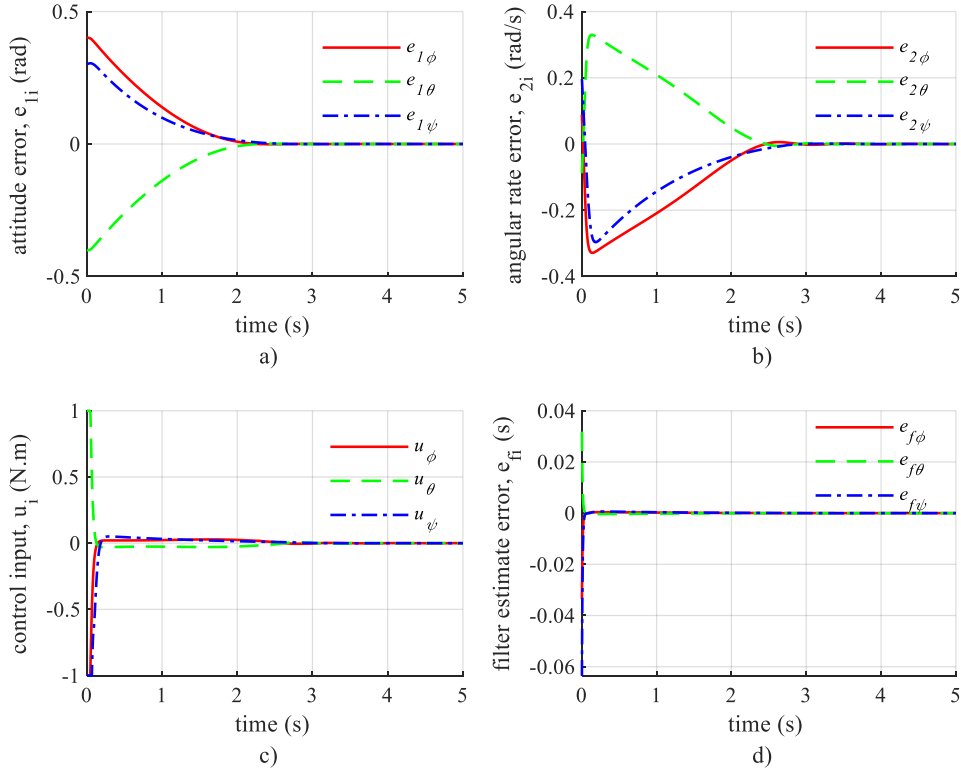


Figure 4. Flight performance of the quadrotor tracking step attitude references. a) The attitude tracking errors rapidly converge to zero without any overshoot; b) The angular rate tracking errors also exhibit fast convergence; c) The controller requires small control effort; d) the filter delivers fast and accurate estimations.

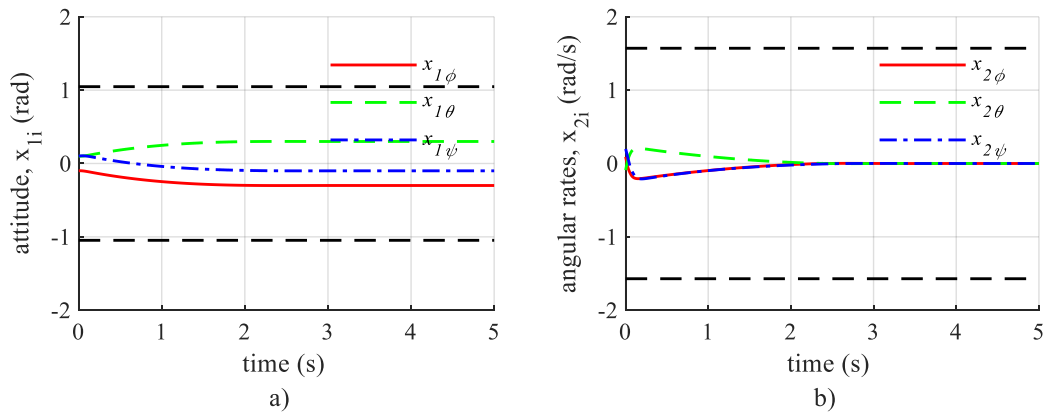


Figure 5. States of the quadrotor tracking step attitude references. The quadrotor's attitude angles (a) and angular rates (b) all lie in the range of the constraints despite having a rapid response.

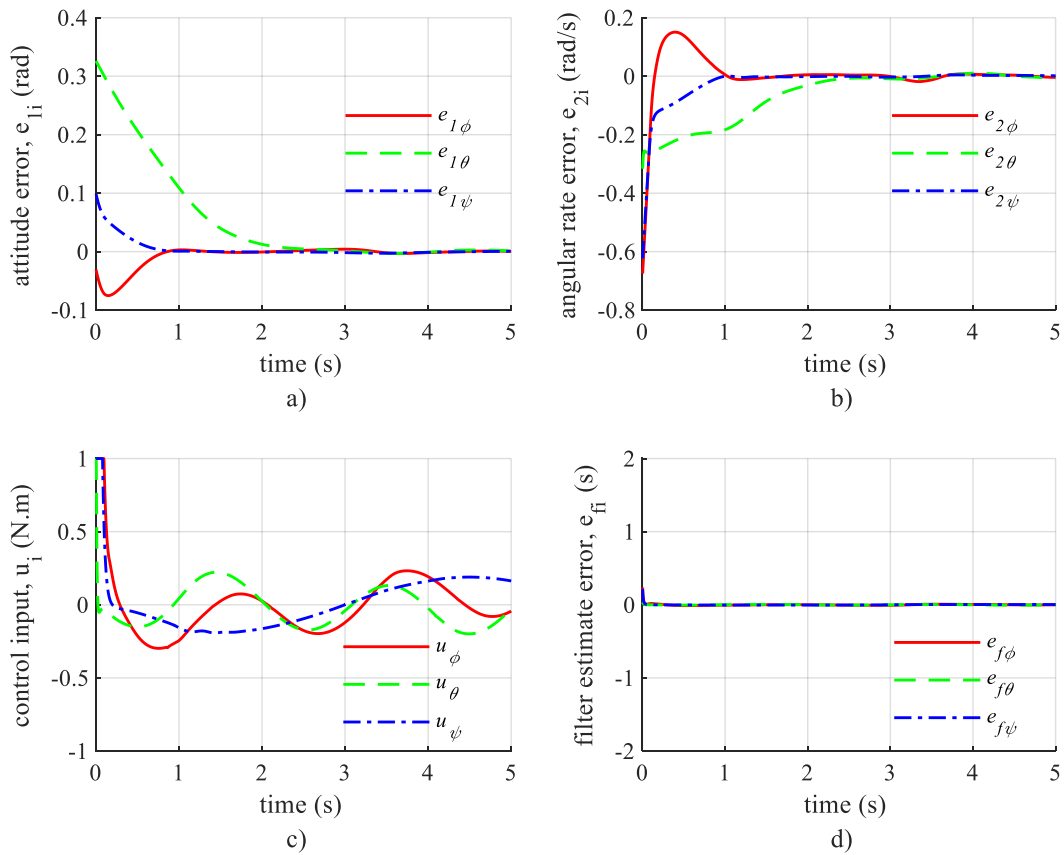


Figure 6. Flight performance of the quadrotor tracking complex and time-varying attitude references. a) The attitude tracking errors rapidly converge to zero; b) The angular rate tracking errors also exhibit fast convergence; c) The controller requires more control effort, but the control inputs are still chattering-free; d) the filter delivers fast and accurate estimations.

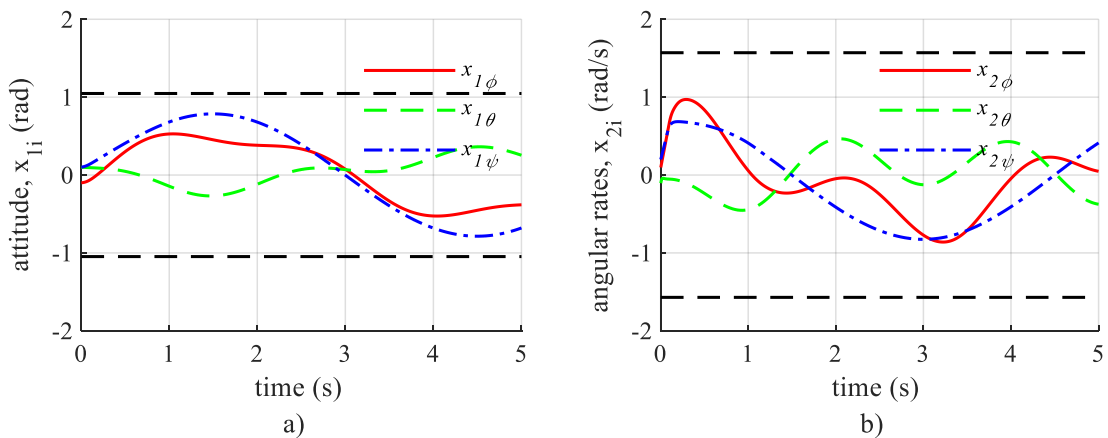


Figure 7. States of the quadrotor tracking complex and time-varying attitude references. The quadrotor's attitude angles (a) and angular rates (b) all lie in the range of the constraints despite having a rapid response.

The second scenario is conducted to ensure the capability of the proposed controller in tracking time-varying references, which are usually fast and complex in most real-world quadrotor missions. As per Table 2, each desired attitude angle is composed of sine waves at different frequencies and amplitudes, which makes it complex and time-varying.

Even though the references vary in a relatively large range of amplitudes, the controller steers the quadrotor to track them rapidly (Figures 6a-b). Depending on the references, the attitude and angular rate tracking errors can converge to zero slightly faster or slower than each other. However, it is seen (Figure 6) that the settling time (2%) does not exceed 2.5 seconds. Compared to the previous scenario, the control inputs see marked increases (Figure 6c). These changes are due to the system requiring larger torques to be able to track the fast-varying references. Nevertheless, the control inputs remain chattering-free. Meanwhile, the filter still works effectively, as its estimation errors take a very short time to reach zero (Figure 6d). This timely estimation allows the backstepping controller properly delivers a fast system response and maintains the system's states not to reach the constraints (Figure 7).

## 5. CONCLUSIONS

This paper addresses the tracking control problem of a quadrotor subject to full-state constraints. By integrating a backstepping control scheme with a fast finite-time filter, the advantages of the backstepping control technique, including rapid response, simple design, and straightforward implementation, are taken while its most significant shortcoming, the “explosion of complexity,” is overcome. The simulation results demonstrate the feasibility and effectiveness of the proposed method in tracking step attitude references and complex time-varying attitude references. The rapid convergence speed and low control effort demand of the controller indicate its applicability in many real-world quadrotor missions. Future work is dedicated to implementing this method into an actual quadrotor and the demonstration in actual flight conditions, in which uncertainties and external disturbances will be considered.

***CRedit authorship contribution statement.*** Mung X. Nguyen: Methodology, Investigation, Funding acquisition, Simulation, Writing, Supervision. Lanh Le Thanh: Formal analysis, Funding acquisition, The Mich Nguyen: Formal analysis, Funding acquisition.

***Declaration of competing interest.*** The authors declare that they have no known competing financial interests or personal relationships that could have appeared to influence the work reported in this paper.

## REFERENCES

1. Idrissi M., Salami M. and Annaz F. - A Review of Quadrotor Unmanned Aerial Vehicles: Applications, Architectural Design and Control Algorithms. *J Intell Robot Syst* **104** (22) (2022). doi.org/10.1007/s10846-021-01527-7.
2. Xuan-Mung N., Nguyen N. P., Nguyen T., Pham D. B., Mai T. V., Ha L.N.N.T., Hong S. K. - Quadcopter precision landing on moving targets via disturbance observer-based controller and autonomous landing planner. *IEEE Access* **10** (2022) 83580-83590. doi.org/10.1109/ACCESS.2022.3197181.
3. Xuan-Mung N., Nguyen N. P., Pham D. B., Dao N. N., Hong S.K. - Synthesized landing strategy for quadcopter to land precisely on a vertically moving apron. *Mathematics*, **10** (2022) 1328. doi.org/10.3390/math10081328.

4. Arif A., Wang H., Castaneda H., and Wang Y. - Finite-Time Tracking of Moving Platform with Single Camera for Quadrotor Autonomous Landing. *IEEE Transactions on Circuits and Systems I: Regular Papers* **70** (2023) 2573-2586, doi:10.1109/TCSI.2023.3256063.
5. Ahmad F., Kumar P., Bhandari A., Patil P. P. - Simulation of the Quadcopter Dynamics with LQR based Control. *Materials Today: Proceedings* **24** (2020) 326-332. doi.org/10.1016/j.matpr.2020.04.282.
6. Xuan-Mung N., Song J.W., Hong S.K. - Quadrotor Robust Optimal Attitude Tracking Control subjected to Model Uncertainties and External Disturbances. 2019 19th International Conference on Control, Automation and Systems (ICCAS), Jeju, 2019, 1450-1453.
7. Das H. - Dynamic Inversion Control of Quadrotor with a Suspended Load. *IFAC-PapersOnLine* **51** (2018) 172-177. doi.org/10.1016/j.ifacol.2018.05.030.
8. Xuan-Mung N., Hong S.K. - Robust Backstepping Trajectory Tracking Control of a Quadrotor with Input Saturation via Extended State Observer. *Applied Science* **9** (2019) 5184. doi.org/10.3390/app9102122.
9. Bangura M., Mahony R. - Real-time Model Predictive Control for Quadrotors. *IFAC Proceedings Volumes* **47** (2014) 11773-11780. doi.org/10.3182/20140824-6-ZA-1003.00203.
10. Sylvain B., Nicolas G., Tarek H., Helene P., Laurent E. - A hierarchical controller for miniature VTOL UAVs: Design and stability analysis using singular perturbation theory. *Control Eng. Pract.* **19** (2011) 1099–1108. doi.org/10.1016/j.conengprac.2011.05.008.
11. Lee J. W., Xuan-Mung N., Nguyen N. P., and Hong S. K. - Adaptive altitude flight control of quadcopter under ground effect and time-varying load: Theory and experiments. *Journal of Vibration and Control* **29** (2023), 571-581. 10.1177/10775463211050169.
12. Khalil H. – *Nonlinear Systems*. Prentice-Hall, Englewood Cliffs, NJ, USA, 2003.
13. Basri M. - Trajectory tracking control of autonomous quadrotor helicopter using robust neural adaptive backstepping approach. *Journal of Aerospace Engineering* **31** (2018) 04017091. doi.org/10.1061/(ASCE)AS.1943-5525.0000804.
14. Zou Y. and Meng Z. - Immersion and invariance-based adaptive controller for quadrotor systems. *IEEE Trans. Syst., Man, Cybern., Syst.* **49** (2018) 2288-2297. doi.org/10.1109/TSMC.2018.2790929.
15. Huang Y. and Xue W. - Active disturbance rejection control: Methodology and theoretical analysis. *ISA Trans.* **53** (2014) 963-976.
16. AbouDonia A., El-Badawy A., and Rashad R. - Active anti-disturbance control of a quadrotor unmanned aerial vehicle using the command filtering backstepping approach. *Nonlinear Dyn.* **90** (2017) 581–597.
17. X. Shao, J. Liu, H. Cao, C. Shen, and H. Wang - Robust dynamic surface trajectory tracking control for a quadrotor UAV via extended state observer. *Int. J. Robust Nonlinear Control* **28** (2018) 2700–2719.
18. Xuan-Mung, N.; Golestani, M. Smooth, Singularity-Free, Finite-Time Tracking Control for Euler–Lagrange Systems. *Mathematics* **10** (2022), 3850. <https://doi.org/10.3390/math10203850>

19. Zuo Z. Y. - Nonsingular fixed-time consensus tracking for second-order multi-agent networks. *Automatica* **54** (2015) 305–309.
20. Q. Hu, B. Jiang, and Y. Zhang - Observer-Based Output Feedback Attitude Stabilization for Spacecraft with Finite-Time Convergence. *IEEE Trans. Cont. Syst. Tech.* **27** (2019) 781-789. doi: 10.1109/TCST.2017.2780061.
21. Polyakov A. - Nonlinear feedback design for fixed-time stabilization of linear control systems. *IEEE Trans. Autom. Control* **57** (2012) 2106-2110.
22. Flame Wheel ARF Kit. Available online: <https://www.dji.com/kr/flame-wheel-arf/spec> (accessed on 1 March 2023).
23. DJI E305. Available online: <http://www.dji.com/product/e305> (accessed on 1 March 2023).